ISSN 0280-5316
ISRN LUTFD2/TFRT--5669--SE

Producing Periodic Motion for Underactuated Systems

Wael Chatila

Department of Automatic Control
Lund Institute of Technology
April 2001

Department of Automatic Control
Lund Institute of Technology
Box 118
SE-221 00 Lund Sweden

Document name
MASTER THESIS

Date of issue
April 2001

Document Number
ISRN LUTFD2/TFRT—5669--SE

Author(s)
Wael Chatila

Supervisor
Rolf Johansson, LTH and Carlos Canudas de Wit, ENSIEG.

Sponsoring organization

Title and subtitle
Producing Periodic Motion for Underactuated Systems. (Gränssvängningar i underaktiverade system).

Abstract

This project considers a special class of aero-dynamics of two different underactuated systems. The two systems under consideration are the Pendubot (actuator at the hip) and the Acrobot (actuator at the knee). The main objectives are to show stability and periodicity of the two systems. The next step is to change the zero-dynamics such that resulting periodic orbits produce walking gait patterns. The stability analysis involves searching for a Lyapunov function which would prove stability and in turn, as can be shown, imply periodicty. The Lyapunov function would also be a powerful help in knowing how to change the zero-dynamics so that desired motions are obtained.
However, a Lyapunov function could not be found, which implies that the succeeding steps are hard to make.

We present in this work some conclusions that would follow from a Lyapunov function and highlight some properties of the systems. We also show how the Pendubot could be brought to upright position.

Keywords

Classification system and/or index terms (if any)

Supplementary bibliographical information

ISSN and key title
0280-5316

ISBN

Language
English

Number of pages
40

Recipient's notes

Security classification

Producing Periodic Motion for Underactuated Systems

Master's Thesis by

Wael Chatila F–96
Department of Automatic Control
Lund, Sweden

Under the supervision of

Rolf Johansson
Department of Automatic Control
Lund, Sweden

Carlos Canudas de Wit
Laboratoire d'Automatique de Grenoble
Grenoble, France

Lund, April 2001

Contents

Chapter 1

Introduction

The systems considered in this project are the two-degree of freedom planar robots, the Pendubot and the Acrobot. They are underactuated, further are the robot links considered to be *rigid* and exhibit *no friction*. The goal is to produce walking gait patterns. *No impact* with the ground is considered at this point. A complete detailed problem formulation will be presented in chapter 2. In this chapter, some definitions of underactuated systems and zero-dynamics are presented. The chapter is concluded with a background on walking mechanisms.

1.1 Underactuated Systems

A system is said to be underactuated when the number of actuators are less than the number of freedom of the system. Underactuated systems present challenging control problems and has recently gained an upswing in research attention. They often exhibit feedforward nonlinearities, nonholonomic constraints and nonminimum phase characteristics, which make them difficult to control and they arise in applications as underactuated marine vehicles, space robots, flexible robots, walking and gymnastic robots such as the pendu- and Acrobot.

A general underactuated n-degree of freedom system with m actuators may be written on the form

$$\begin{aligned} D_{11}(\mathbf{q})\ddot{\mathbf{q}}_{\mathbf{1}} + D_{12}(\mathbf{q})\ddot{\mathbf{q}}_{\mathbf{2}} + F_1(\mathbf{q},\dot{\mathbf{q}})\dot{\mathbf{q}} &= B(q)\mathbf{u} \\ D_{21}(\mathbf{q})\ddot{\mathbf{q}}_{\mathbf{1}} + D_{22}(\mathbf{q})\ddot{\mathbf{q}}_{\mathbf{2}} + F_2(\mathbf{q},\dot{\mathbf{q}})\dot{\mathbf{q}} &= 0 \end{aligned}$$

where $q \in \mathbf{R^n}$ are the generalized coordinates, $q_1 \in \mathbf{R^m}$, $q_2 \in \mathbf{R^{n-m}}$, $B \in \mathbf{R^{mxm}}$ invertible $\forall q$, D_{ij} components of the $\mathbf{R^{nxn}}$ inertia matrix. For further descriptive description of different properties and results please refer to [3] and [4].

There have been some progress in controlling and analyzing underactuated systems with passivity and energy approaches. See [8] and [6]

1.2 Zero-dynamics

The zero-dynamics of a system is the resulting dynamics of the system when it is moving on the manifold $Z^* = \{x \mid y = 0\}$ when

$$\begin{aligned} \dot{x} &= f(x) + g(x)u \\ y &= h(x) \end{aligned} \tag{1.1}$$

where $f(x), g(x)$ and $h(x)$ represents general nonlinear functions, x is the state vector. In the case of a *linear* system the zero-dynamics is strongly associated with the zeros of its transfer function. If there exist zeros in the right-half plane of the minimal realization of a linear system's transfer function, thus having nonminimum-phase, the zero-dynamics would be unstable. Vice verse, if the system is minimum-phase, having zeros only in the left-half plane, the zero-dynamics are stable.
Whenever $\forall x \in Z^* \Rightarrow h(x) = 0$ there exists an unique u^* such that

$$\dot{x} = f^*(x) = f(x) + g(x)u^*, \quad x \in Z^* \quad \forall t \tag{1.2}$$

A nonlinear system is said to be in *nonminimum-phase* at x_{eq}, if x_{eq} is an unstable equilibrium point of $f^*(x)$, otherwise it is in minimum-phase at x_{eq} [9].

1.3 Background on walking mechanisms

The work done by McGeer in [10],[13] show how a 2D-biped robot with *no actuator* what so ever and hence *no control* can produce human like gait patters, whose only source of energy is gravity on a downhill slope. His idea was that of the Wright brothers when discovering how to fly. The Wright brothers, the aviation pioneers, first developed airplanes without motors and mastered the fundamental of aerodynamics. Then, after successfully having constructed gliders they attached motors.
Studies of human gait [15] also show that the legs' muscles are primarily active during the support and the takeoff phase and most of the time the legs are more or less like a free double pendulum.

Chapter 2

Problem formulation

2.1 General equations of motions

The general equations of motion for any n-degree of freedom mechanical system are

$$D(\mathbf{q})\ddot{\mathbf{q}} + C(\mathbf{q}, \dot{\mathbf{q}})\dot{\mathbf{q}} + G(\mathbf{q}) = B(\mathbf{q})\tau = B(\mathbf{q}) \begin{pmatrix} \tau_1 \\ \tau_2 \\ \vdots \\ \tau_n \end{pmatrix}$$

Where τ is the input torque and $q \in R^n$ are the generalized coordinates. For our two systems under consideration $n = 2$, further the Pendubot has $\tau = \begin{pmatrix} \tau_1 \\ 0 \end{pmatrix}$, and the Acrobot, $\tau = \begin{pmatrix} 0 \\ \tau_2 \end{pmatrix}$, we have

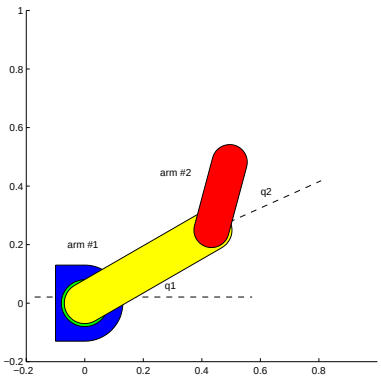

Figure 2.1:

$$D = \begin{pmatrix} d_{11} & d_{12} \\ d_{21} & d_{22} \end{pmatrix} = \begin{pmatrix} J_1 + J_2 + 2J_3 \cos q_2 & J_2 + J_3 \cos q_2 \\ d_{12} & J_2 \end{pmatrix}$$

$$C = \begin{pmatrix} c_{11} & c_{12} \\ c_{21} & c_{22} \end{pmatrix} = -J_3 \sin q_2 \begin{pmatrix} \dot{q}_2 & \dot{q}_1 + \dot{q}_2 \\ -\dot{q}_1 & 0 \end{pmatrix}$$

$$G = \begin{pmatrix} g_1 \\ g_2 \end{pmatrix} = \begin{pmatrix} gJ_4 \cos q_1 + gJ_5 \cos(q_1 + q_2) \\ gJ_5 \cos(q_1 + q_2) \end{pmatrix}$$

J_1	$m_1 l_{c1}^2 + m_2 l_1^2 + I_1$
J_2	$m_2 l_{c2}^2 + I_2$
J_3	$m_2 l_1 l_{c2}$
J_4	$m_1 l_{c1} + m_2 l_1$
J_5	$m_2 l_{c2}$
m_i	*mass* of link i
l_i	*length* of link i
l_{ci}	length from the previous joint to *center of mass* of link i
D	*Inertia matrix*
C	*Coriolis matrix*
G	*Gravity matrix*

The variables q_1 and q_2 are defined according to Fig. 2.1 above. Values of above parameters used in simulations are
$m_1 = 6\ kg$, $m_2 = 4\ kg$, $l_1 = 0.52\ m$, $l_2 = \textit{never used}$, $l_{c1} = 0.3\ m$, $l_{c2} = 0.29\ m$, $g = 9.81\ m/s^2$, $I_1 = I_2 = 0\ kg \cdot m^2$. These values correspond to a lab robot at I.N.R.I.A.[1] In the above equations the robot links and joints are assumed to be rigid and frictionless.

2.2 Zero dynamics

In this project we study the resulting motion when $h(x) \equiv e(q) = q_1 - aq_2 - b = 0$ in (1.1), $a, b \in R$. Thus replacing q_1, $\dot{q}_1$ and $\ddot{q}_1$ with $q_1 = aq_2 + b$, $\dot{q}_1 = a\dot{q}_2$ and $\ddot{q}_1 = a\ddot{q}_2$, respectively. The new set of equations become

$$\begin{cases} (ad_{11} + d_{12})\ddot{q}_2 + (ac_{11} + c_{12})\dot{q}_2 + g_1 \equiv \bar{d}_1 \ddot{q}_2 + \bar{c}_1 \dot{q}_2^2 + g_1 = \tau_1 \\ (ad_{12} + d_{22})\ddot{q}_2 + (ac_{21} + c_{22})\dot{q}_2 + g_2 \equiv \bar{d}_2 \ddot{q}_2 + \bar{c}_2 \dot{q}_2^2 + g_2 = \tau_2 \end{cases} \tag{2.1}$$

Putting either one of $\tau_i = 0$ and using $x_1 = q_2$ we get

$$\begin{cases} \dot{x}_1 = x_2 \\ \dot{x}_2 = -\frac{1}{\bar{d}_i}(\bar{c}_i x_2^2 + g_i) \end{cases}$$

[1] Institut National de Recherche en Informatique et en Automatique, Grenoble, France http://www.inrialpes.fr

For the case $\tau_2 = 0$ (Pendubot) the above equations are

$$\begin{cases} \dot{x}_1 = x_2 \\ \dot{x}_2 = -\frac{a^2 J_3 x_2^2 \sin x_1 + g J_5 \cos((a+1)x_1 + b)}{(a+1)J_2 + a J_3 \cos x_1} = -\frac{a^2 m_2 l_1 l_{c2} x_2^2 \sin x_1 + g m_2 l_{c2} \cos((a+1)x_1 + b)}{(a+1)m_2 l_{c2}^2 + a m_2 l_1 l_{c2} \cos x_1} \\ u^* = \tau_1^* = \dot{x}_1^2(\bar{c}_1 - \bar{c}_2 \frac{\bar{d}_1}{\bar{d}_2}) + g_1 - g_2 \frac{\bar{d}_1}{\bar{d}_2} \end{cases} \tag{2.2}$$

And for the case $\tau_1 = 0$ (Acrobot) the above equations are

$$\begin{cases} \dot{x}_1 = x_2 \\ \dot{x}_2 = \frac{(2a+1)m_2 l_1 l_{c2} x_2^2 \sin x_1 - g(m_1 l_{c1} + m_2 l_1)\cos(a x_1 + b) - g m_2 l_{c2} \cos((a+1)x_1 + b)}{a(m_1 l_{c2}^2 + m_2(l_1^2 + l_{c2}^2)) + m_2 l_{c2}^2 + (2a+1)m_2 l_1 l_{c2} \cos x_1} \\ u^* = \tau_2^* = \dot{x}_1^2(\bar{c}_2 - \bar{c}_1 \frac{\bar{d}_2}{\bar{d}_1}) + g_2 - g_1 \frac{\bar{d}_2}{\bar{d}_1} \end{cases} \tag{2.3}$$

It is these two above (zero-dynamical) systems of equations (2.2) and (2.3) that are the subject of our attention for the rest of this work.

Chapter 3

Investigation of the zero-dynamics

3.1 Linearization

The equilibria for the Pendubot are given by

$$\begin{cases} x_2 = 0 \\ \\ cos((a+1)x_1 + b) = 0 \Rightarrow x_1^* = \frac{\frac{\pi}{2}(1+2k)-b}{a+1} \end{cases} \tag{3.1}$$

And for the Acrobot by

$$\begin{cases} x_2 = 0 \\ \\ (m_1 l_{c1} + m_2 l_1)\cos(ax_1 + b) + m_2 l_{c2}\cos((a+1)x_1 + b) = 0 \end{cases} \tag{3.2}$$

Linearisation around the equilibria yield the following structure

$$\dot{x} = Ax = \begin{pmatrix} 0 & 1 \\ -\alpha & 0 \end{pmatrix} x \tag{3.3}$$

Thus when $\alpha < 0$ the eigenvalues will be on the real axis and (unstable) saddle points. When $\alpha > 0$ eigenvalues will be on the imaginary axis and are neutral stable equilibra (centers) which can be shown be considering the following Lyapunov function valid for the linearized system.

$$V = \frac{1}{2}(\alpha x_1^2 + x_2^2) \Longrightarrow \dot{V} = \alpha x_1 \dot{x}_1 + x_2 \dot{x}_2 = \alpha x_1 x_2 - x_2 \alpha x_1 = 0 \tag{3.4}$$

For the Pendubot (3.1), saddles will exist at $k = 0, \pm 2, \pm 4, \ldots$

3.2 Bounded orbits are periodic

If solutions to (2.2) and (2.3) are bounded then their positive limit sets[1] can not contain any equilibria. This, because a solution can never reach a center and of

[1] see section A.2 for definition of positive limit sets.

course never reach a saddle. To show the former statement and assuming the system is Lipschitz, we consider the orbits in a sufficiently small ball of radius ϵ so that the linearized system (3.3) holds. Then the Lyapunov function (3.4) holds which imply that no orbit can asymptotically reach an equilibrium. Thus all condition for the Poincaré-Bendixson theorem (A.3) are fulfilled.

The systems (2.2) and (2.3) also have the property that they are time reversible[2] implying that bounded orbits are symmetric with respect to the x_1-axis and that they also must cross the x_1-axis only twice.

3.3 Simulations of the systems

In this section some simulation results that could shade some light of the different effects the parameters a, b and initial start condition x_0 have on (2.2) and (2.3) are presented. Simulations were carried out using MATLAB/SIMULINK.

3.3.1 Limitations on a and b

For the systems to have periodic solutions we demand that the denominators in (2.2) and (2.3) are separated from zero $\forall t$. For the Pendubot case this is fulfilled if $-0.35 = -\frac{\varepsilon}{1+\varepsilon} < a < \frac{\varepsilon}{1-\varepsilon} = 1.26$, where $\varepsilon = \frac{l_{c2}}{l_1} < 1$. And for the Acrobot the limits on a are $-0.30 = -\frac{\pi_3+\pi_2}{\pi_1+2\pi_3} < a < \frac{\pi_3-\pi_2}{\pi_1-2\pi_3} = 0.37$, where $\pi_1 = m_1 l_{c2}^2 + m_2(l_{c2}^2 + l_1^2)$, $\pi_2 = m_2 l_{c2}^2$, $\pi_3 = m_1 l_1 l_{c2}$.

It can also be shown that equilibria will be saddles and centers on every other position for the Pendubot. The parameter b can be chosen arbitrary as far as singularities are concerned.

[2] A system is said to be time reversible if orbits in forward and backward time look the same. With other words, we can not differentiate a movie of the system when played backwards or forwards. To prove time reversible use $t := -t \Longrightarrow x_1 := x_1, \dot{x}_1 := -\dot{x}_1, x_2 := -x_2, \dot{x}_2 := \dot{x}_2$. Putting these expressions into (2.2) and (2.3) we find the result to be identical to the original systems, indicating that the motion looks the same in forward and backward time.

3.3.2 Pendubot

Variation of x_0

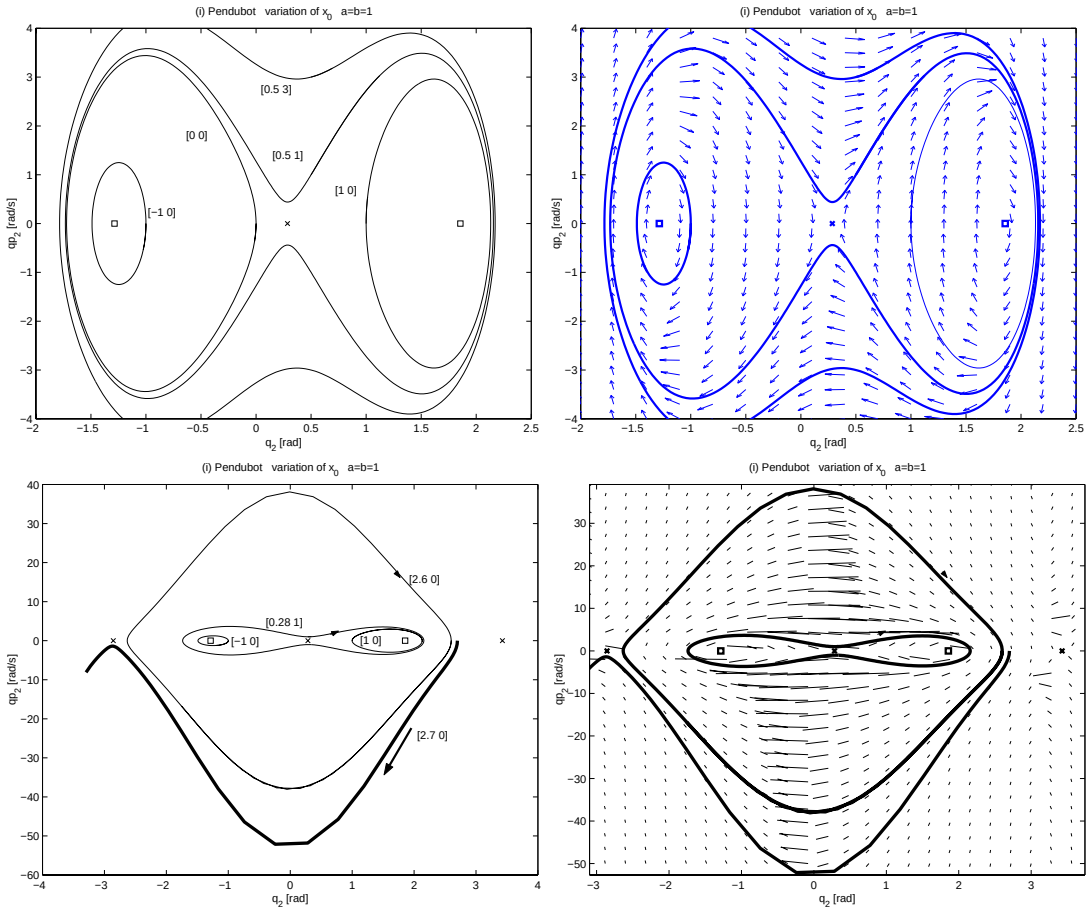

Figure 3.1: Variation of initial condition of $x_0 = [q_2 \ \dot{q}_2]'$, $a = b = 1$. Bottom, zoom out of the top plots. The [2.7 0] orbit seem not to be a closed curve and is in fact unbounded with respect to x_1.

Variation of a

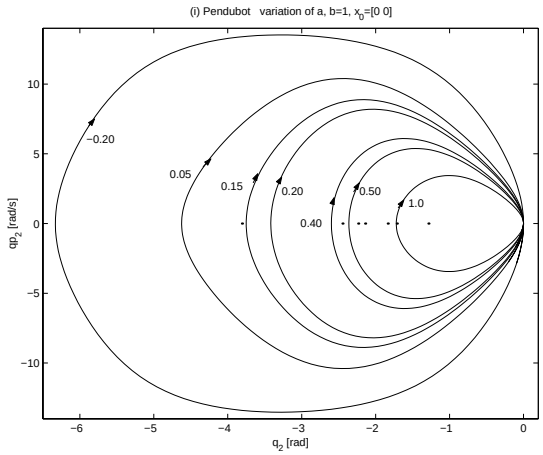

Figure 3.2: Variation of a. The small dots indicate the positions of centres.

Variation of b

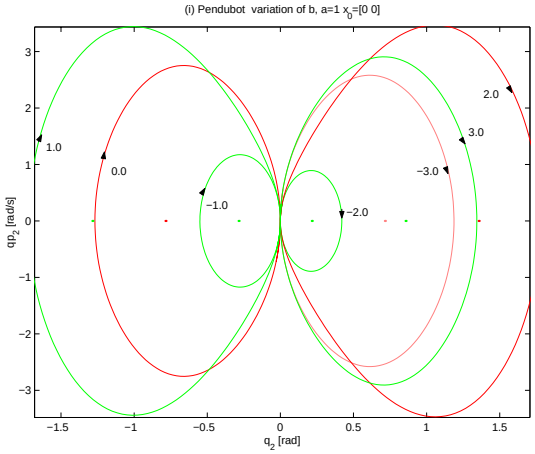

Figure 3.3: Variation of b. The orbits $b = 1$, $b = 2$ reveals an important property of the system. The effect on the system when changing b is nothing else than shifting the equilibria, thus shifting the whole system.

3.3.3 Acrobot

Variation of x_0

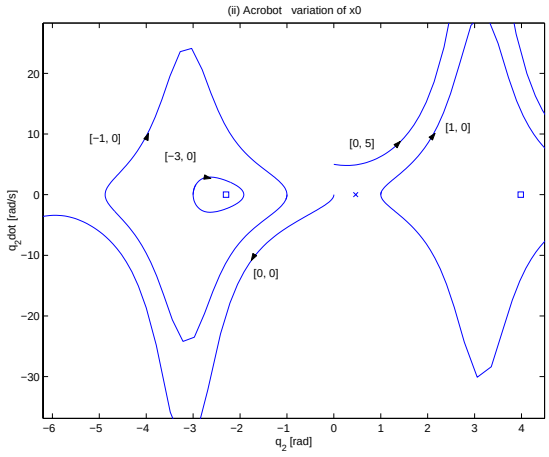

Figure 3.4: Variation of $x_0 = [q_{02}\ \dot{q}_{02}]$. $a = b = 1$.

Variation of a

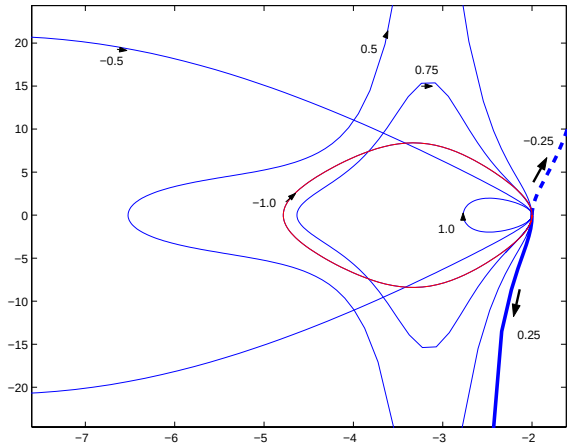

Figure 3.5: Variation of a. $x_0 = [q_{02}\ \dot{q}_{02}] = [-2\ 0]$,$b = 1$

Variation of b

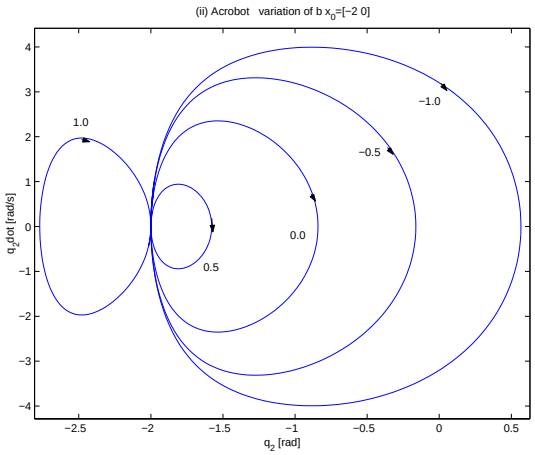

Figure 3.6: Variation of b. $x_0 = [q_{02}\ \dot{q}_{02}] = [-2\ 0]$,$a = 1$

3.4 An observation

By letting $b = \frac{\pi}{2}$ then, for the Pendubot, we can always find (shown empirically) an orbit that, at some point, intersects the x_2-axis. This means that at that point, $x_1 = q_2 = 0 \Rightarrow q_1 = aq_2 + b = b = \frac{\pi}{2}$. This configuration corresponds to the upright position for the robot. Thus, succeeding in rendering the the Pendubot into the zero-dynamics and to an orbit that intersects the x_2-axis at some point in the zero-dynamics, the Pendubot could be brought to upright position.

This result has some drawbacks. Since there is no formal proof for stability of the zero-dynamics and its corresponding region of stability, there could be some unaccepted problems. Also we can not decide which orbit in the zero-dynamics the system will go to.

3.5 Summary & Conclusions

For the Pendubot, the effect of the b-parameter is that of *shifting* the equilibria and hence does not change any basic property of the system. The a-parameter has no easily comprehensible effect. Although one can perhaps believe, by inspecting (2.2), that by increasing a introduce more nonlinearities.

The effect of the initial start condition x_0 decide the destiny of the future orbits which can be either stable or unstable.

In the case of the Acrobot things are a harder to analyze because of the strong nonlinearities. Hence most of the work and results are valid only for the Pendubot.

Chapter 4

Searching for a Lyapunov function – Trials

In this chapter different approaches and trials to find a Lyapunov, which never was found, are presented. By finding a Lyapunov function for the systems (2.2) and (2.3) we can proceed to predict a region in the phase plane as a function of a and b where solutions will be bounded. Boundedness would also imply periodicity as showed in section (3.2).

From simulations we can draw the conclusion that if we can find a Lyapunov function, $V(\mathbf{x})$, then we must have $\dot{V}(\mathbf{x}) = 0$.

4.1 Energy

Usually the total energy of a mechanical systems fulfills the requirement of a Lyapunov function. However this approach does not work, since the total mechanical energy of the zero-dynamical system is not constant.

By going further on the path of energy and modifying the total energy function by adding a term that correspond to the energy input, we can find a function which time derivative would equal to zero:

Consider first the Lyapunov function candidate (the total energy)

$$\bar{V} = \frac{1}{2}\dot{q}^T D\dot{q} + P \Longrightarrow \dot{\bar{V}} = \dot{q}_i u_i^* \neq 0$$

P is the potential energy. Consider now the following Lyapunov function candidate

$$V = \frac{1}{2}\dot{q}^T D\dot{q} + P - \int_0^t \dot{q}_i u_i^* dt \neq 0 \implies \dot{V} \equiv 0 \tag{4.1}$$

The problem is of course to evaluate the time integral. A good try is using the relation

$$\int_0^t \dot{q}_i u_i^* dt = \int_{q_i(0)}^{q_i(t)} u_i^*(q_i, \dot{q}_i) dq_i \tag{4.2}$$

but useless because of the existence of $\dot{q}_i$ terms/factors in $u_i^*(q_i, \dot{q}_i)$. Even if we somehow could integrate the above expression we would run into an other

problem... we conclude by studying (4.1) that V will take the constant value corresponding to the initial energy, i.e. $V(t) = V(0) = E_{tot}(0)$, $\forall t$. Now, if we start on the x_1-axis (initial velocity equals zero) the initial and all future values of V would depend only on the initial potential energy. Numerical integration of the expression in (4.2) shows indeed that for a given start value V will remain constant and take the value equal to the initial energy. So far so good but, starting on different points on an orbits we would expect to get the same constant V, however this is not the case. Below a figure of two different simulations starting on different points on the same orbit. The explanation for

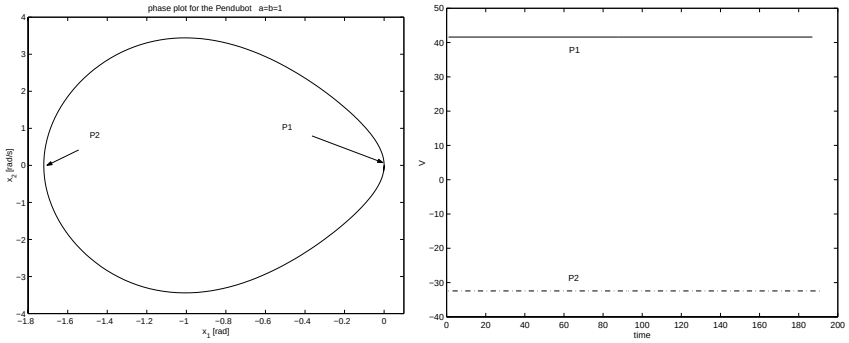

Figure 4.1: Pendubot case. The values of $V(t)$ starting at P1 and P2.

this is of course that the potential energy at P1 and P2 are different.

In connection with this there was an idea to change either a or b in a Poincaré type of section on the x_1-axis in order to make sudden (discontinuous) jumps to a desired orbit. But this could not work when examining following figure. Changing a or b abruptly at a point, say $x_s(t)$, is equivalent to stopping a sim-

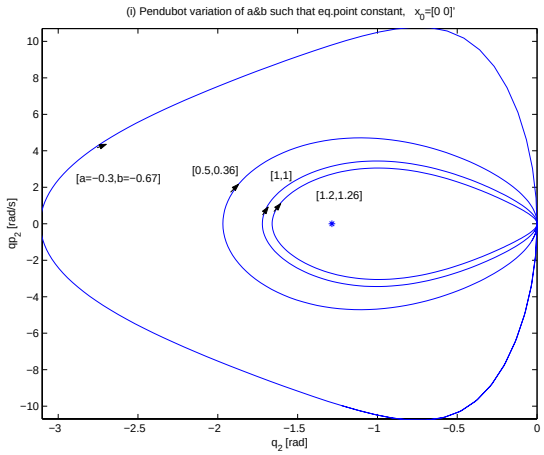

Figure 4.2: Pendubot. Changing a and b such that equilibria are the same, always starting in $x_0 = [0\ 0]'$.

ulation at x_s, changing parameters and then continuing the simulation with x_s as initial condition. The result will be that orbits at x_s will be tangential to each other and thus the idea that we could make a jump will not work (compare the double integration of a spike).

4.2 Lagrangian form

In many cases, the Lagrangian of a system will fulfill the requirements of a Lyapunov function. The Lagrangian is defined by the function $L = K - P$, (K-kinetic energy, P-potential energy), that fulfills the relation

$$\frac{d}{dt}\{\frac{\partial L}{\partial \dot{q}}\} - \frac{\partial L}{\partial q} = 0 \tag{4.3}$$

The kinetic energy is calculated from the expression $K = \frac{1}{2}\dot{q}^T M \dot{q}$. For our zero-dynamical systems M corresponds to $\bar{d}_i$ in (2.1) and P to g_i. Using these identities we find that they do not fulfill the relation (4.3), and the zero-dynamics could thus not be written on Lagrangian form.

4.3 Transformation to a circle

According to a result in [12], there exists for every closed orbit a transformation of coordinates to a circle, i.e.

$$\left\{ \begin{array}{l} \dot{x}_1 = x_2 \\ \dot{x}_2 = f(x) \end{array} \right. \overset{y=T(x)}{\longrightarrow} \left\{ \begin{array}{l} \dot{y}_1 = \alpha y_2 \\ \dot{y}_2 = -\alpha y_1 \end{array} \right.$$

A Lyapunov function can then trivially be found for the 'circle'-system, then by transforming back to the old coordinates we would have our Lyapunov function. However, to find such a transformation, $T(x)$, is a problem in itself. We need to solve the following system of partial differential equations, $f(x)$ is the expression for $\dot{x}_2$ in (2.2) or (2.3)

$$\left\{ \begin{array}{l} y_1 = T_1(x) \\ y_2 = T_2(x) \end{array} \right. \Leftrightarrow \left\{ \left(\begin{array}{c} \dot{y}_1 \\ \dot{y}_2 \end{array} \right) = \left[\frac{\partial T}{\partial x} \right] \dot{x} = \left[\begin{array}{cc} \frac{\partial T_1}{\partial x_1} & \frac{\partial T_1}{\partial x_2} \\ \frac{\partial T_2}{\partial x_1} & \frac{\partial T_2}{\partial x_2} \end{array} \right] \left(\begin{array}{c} x_2 \\ f(x) \end{array} \right) \Leftrightarrow \right.$$

$$\Leftrightarrow \left\{ \begin{array}{rcl} \frac{\partial T_1}{\partial x_1} x_2 + \frac{\partial T_1}{\partial x_2} f(x) & = & \alpha T_2 \\ \frac{\partial T_2}{\partial x_1} x_2 + \frac{\partial T_2}{\partial x_2} f(x) & = & -\alpha T_1 \end{array} \right.$$

...which we could not solve. This of course raise the question if there exist an analytic solution to the above system of PDE, and if on the whole there exist an analytic Lyapunov function?

Chapter 5

Changing b to steer the zero-dynamics

By inspecting (2.2) and (2.3), presented again below, one could by choosing a appropriately (small) linearize the equations through b.

$$\begin{cases} \dot{x}_1 = x_2 \\ \\ \dot{x}_2 = -\frac{a^2 J_3 x_2^2 \sin x_1 + g J_5 \cos((a+1)x_1 + b)}{(a+1)J_2 + a J_3 \cos x_1} \end{cases}$$

For the Pendubot the expression for b, by mere inspection becomes

$$b = \arccos[\frac{((a+1)J_2 + aJ_3 \cos x_1)(k_1(x_1 - x_1^d) + k_2 x_2) - a^2 J_3 x_2^2 \sin x_1}{g J_5}] - (a+1)x_1 \tag{5.1}$$

which always will be well defined assuming a, k_1, k_2, J_2, J_5 can be chosen appropriately. The resulting (linearized) system then becomes

$$\begin{cases} \dot{x}_1 = x_2 \\ \\ \dot{x}_2 = -k_1(x_1 - x_1^d) - k_2 x_2 \end{cases} \tag{5.2}$$

which is globally exponentially stable.

5.1 The Swing up of the Pendubot in the zero-dynamics by changing b

For the Pendubot robot arms to swing up in upright position, q_1 and q_2 must tend to $q_1 = \frac{\pi}{2}$ and $q_2 = 0$, respectively. Thus $x_1^d = 0$ in (5.1) and (5.2). Observing that when

$$x_1 \to 0 \quad \Rightarrow \quad x_2 \to 0 \quad \Rightarrow \quad b \to \pm\tfrac{\pi}{2} \quad \Rightarrow \quad q_1 \to \pm\tfrac{\pi}{2}$$

since $q_1 = aq_2 + b$. Below a simulation when changing b according to (5.1).

We can note that the system has low damping and low bandwidth. This, of course because k_2 $(= 2\omega_0\xi)$ and k_1 $(= \omega_0^2)$ in (5.1) must be small to keep the magnitude of the argument of arccos less than one.

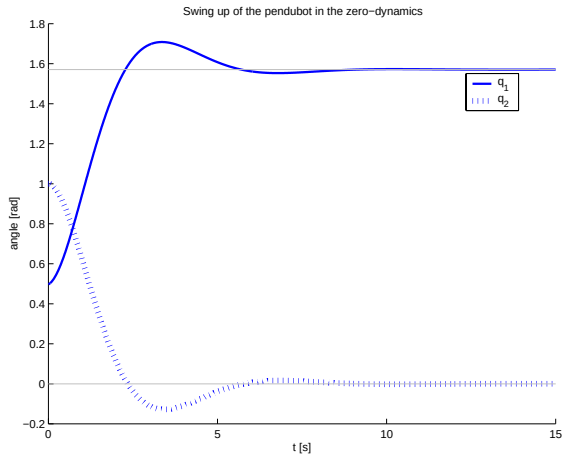

Figure 5.1: Variation of b to get the Pendubot in upright position. The values of q_1 are calculated through $q_1(t) = aq_2(t) + b(t)$

In general, for any x_1^d it can easily be shown that $q_1 + q_2 = \pm\frac{\pi}{2}$ when $t \to \infty$. This means that the suggested control strategy can put the Pendubot into "any" configuration provided $q_1 + q_2 = \pm\frac{\pi}{2}$.

5.2 Producing periodic motions by changing b

One of the goals of this project is to prove and produce periodic motion. By the technique in the previous section this can easily be done. For example, the system in (5.1) can be linearized so the equations become those of a harmonic oscillator.

$$\begin{cases} \dot{x}_1 = x_2 \\ \dot{x}_2 = -kx_1 \end{cases}$$

However, by doing this the main idea by letting $q_1 = aq_2 + b$ is somehow lost.

Chapter 6

Forcing the system into the zero-dynamics

Everything that have been said and done previously is nothing else than science-fiction until we try to force the (full) system into the zero-dynamics, i.e. $q_1^d = aq_2 + b$.

The equations for the Pendubot of full system are once again

$$\begin{cases} d_{11}\ddot{q}_1 + d_{12}\ddot{q}_2 + h_1 = \tau_1 \\ \\ d_{21}\ddot{q}_1 + d_{22}\ddot{q}_2 + h_2 = 0 \end{cases} \tag{6.1}$$

were coriolis and gravity forces have been written on the more compact form h_i. We want q_1 to follow a given trajectory, namely that of $q_1 = aq_2 + b$. This could be done by using *partial feedback linearization*. From the second expression in (6.1) we get

$$\ddot{q}_2 = \frac{1}{d_{22}}(-d_{12}\ddot{q}_1 - h_2) \tag{6.2}$$

substituting this expression in the first equation of (6.1), we get

$$(d_{11} - \frac{d_{12}^2}{d_{22}})\ddot{q}_1 + (h_1 - \frac{d_{12}}{d_{22}}h_2) = \bar{d}\ddot{q}_1 + \bar{h} = \tau_1 \tag{6.3}$$

From properties of the inertia matrix it follows that $\bar{d} > 0$. Thus a partial feedback linearization can be done according to

$$\tau_1 = \bar{d}\nu + \bar{h} \quad \Rightarrow \quad \ddot{q}_1 = \nu$$

Using the control law

$$\nu = \ddot{q}_1 = \ddot{q}_1^d + k_v(\dot{q}_1^d - \dot{q}_1) + k_p(q_1^d - q_1) \tag{6.4}$$

will render the system exponentially fast to the zero-dynamics.

6.1 Forcing the system into the zero-dynamics when a & b are fixed

When a and b are fixed we have

$$\begin{cases} q_1^d = aq_2 + b \\ \dot{q}_1^d = a\dot{q}_2 \\ \ddot{q}_1^d = a\ddot{q}_2 \end{cases} \tag{6.5}$$

Substituting these expression in (6.4) and using (6.2) we get

$$\begin{aligned} \ddot{q}_1 &= a\ddot{q}_2 + k_v(a\dot{q}_2 - \dot{q}_1) + k_p(aq_2 + b - q_1) = \\ &= \tfrac{a}{d_{22}}(-d_{12}\ddot{q}_1 - h_2) + k_v(a\dot{q}_2 - \dot{q}_1) + k_p(aq_2 + b - q_1) \\ &\Leftrightarrow \\ (\tfrac{ad_{12}}{d_{22}} + 1)\ddot{q}_1 &= k_v(a\dot{q}_2 - \dot{q}_1) + k_p(aq_2 + b - q_1) - \tfrac{ah_2}{d_{22}} \\ &\Leftrightarrow \\ \nu = \ddot{q}_1 &= \tfrac{d_{22}(k_v(a\dot{q}_2 - \dot{q}_1) + k_p(aq_2 + b - q_1)) - ah_2}{ad_{12} + d_{22}} \end{aligned}$$

which will be well defined when $ad_{12} + d_{22} > 0$, which is the same expression appearing in the denominatior of (2.2)

To show that this control law works, a simulation in the zero-dynamical system is compared with a simulation of the full system when forcing it into the same zero-dynamics.

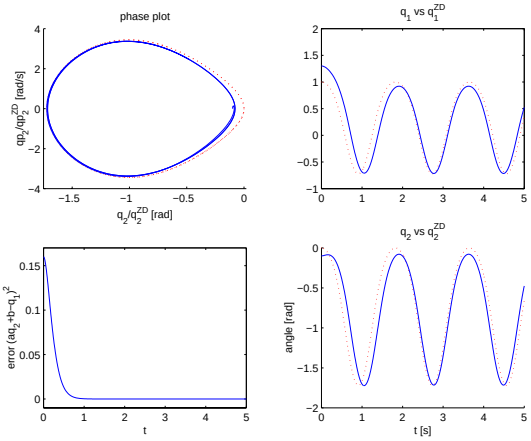

Figure 6.1: Forcing the system into the zero-dynamics. Solid line is the full system. $a = b = 1$, $x_0 = [0\ 0]'$, $w_0 = 5$ and $\xi = 1$ in (6.4). The explanation for the difference between the two cases is, starting a bit off the zero-dynamics will imply a different x_0. However, starting exactly in the zero-dynamics, the two cases will be identical.

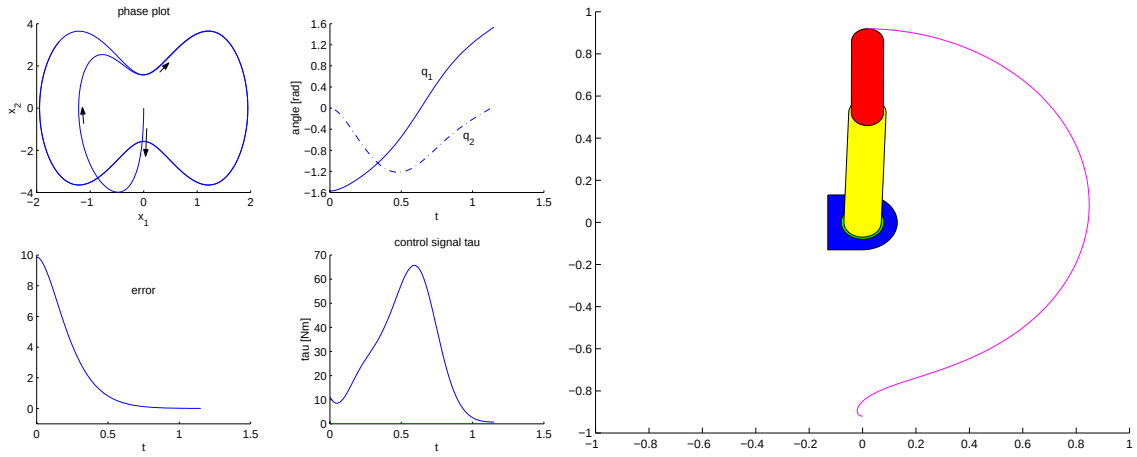

Figure 6.2: Swing up of the Pendubot. $a = 1$, $b = \frac{\pi}{2}$, $\omega_0 = 5$ and $\xi = 1$.

In Sec. 3.4 an idea to swing up the Pendubot was presented. Above, a simulation with the full system when $a = 1$, $b = \frac{\pi}{2}$. The system reaches upright position, but to keep it there, it is necessary to switch to an other controller that would keep it there. Such a controller is discussed in [11] where the controller design is performed with LQR which provides local exponential stability. The disadvantage of our control strategy is the need of high-torque actors and the uncertainty of the behavior of future orbits.

In the above simulation we have gone from downright position to upright. A variety of start configurations have been simulated that would take the robot to upright position. For the robot to go to upright position the limit cycles have to be outside the curve presented in Fig. 6.3. Starting *exactly* in the zero-dynamics for an orbit that goes outside the curve in Fig. 6.3 would solve the latter problem presented above. The necessity for a high-torque actor is the requirement to be able to reproduce the signal u^* in (2.2), which for some zero-dynamical orbits produce high torques.

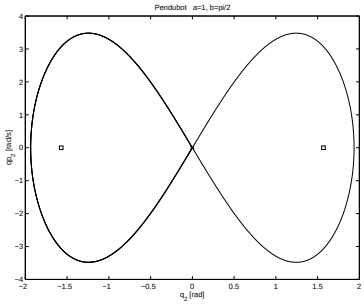

Figure 6.3: If limit cycles are outside the curve, then the robot arm will tend to upright position (limit cycle must intersect the x_2-axis). The curves have been created by first starting a little to the left, and then a little to the right of the saddle point at $(0, 0)$.

6.2 Forcing the system into the zero-dynamics when b is changing

In (5.1), a must be small to cope with the x_2^2 term. To simplify the following discussion we could let $a = 0$. The simplified expression for b now looks

$$b = \arccos(\frac{J_2}{gJ_5}(k_1(x_1 - x_1^d) + k_2 x_2)) - x_2$$

Using $q_1^d = b$, (6.4) becomes

$$\nu = \ddot{q}_1 = \ddot{b} + k_v(\dot{b} - \dot{q}_1) + k_p(b - q_1)$$

This give raise to two fundamental questions. How to calculate $\dot{b}$ and $\ddot{b}$? and if we derived the equations for the zero-dynamics under the assumption that b was a constant, then could we expect to be able to force the system into the zero-dynamics when changing b continuously according to (5.1)? The answer must be no.

Chapter 7

Experimental results

Experiments were carried out in Lund on a Pendubot developed by [11].

7.1 Experimental setup

The Pendubot used in the experiments has the following design.

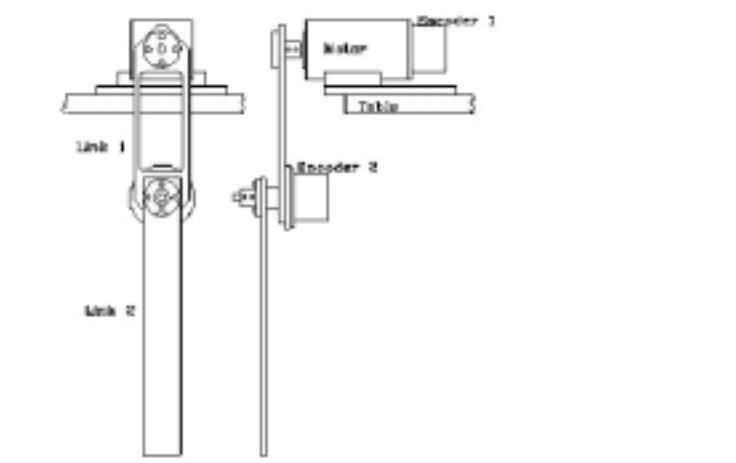

Figure 7.1:

Identification of the parameters J_i carried out in [11] resulted in the estimation

J_1	0.09	$kg \cdot m^2$
J_2	0.025	$kg \cdot m^2$
J_3	0.0214	$kg \cdot m^2$
J_4	0.44	$kg \cdot m$
J_5	0.11	$kg \cdot m$

Further we neglect friction, non-rigid effects and possible motor dynamics. Since the angular velocities are not available for measurement we are forced to use an observer. The installation with the observer and controller is presented in Fig. 7.1 below.

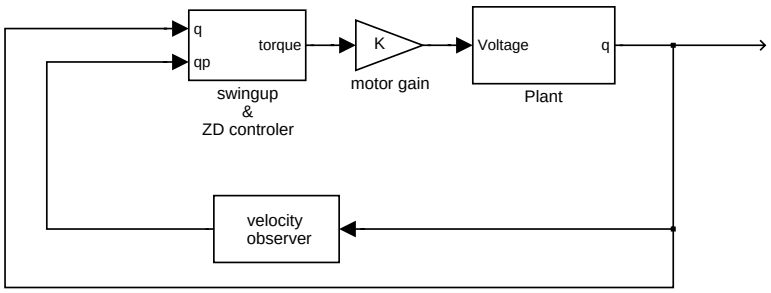

Figure 7.2:

7.2 Preliminary Simulations

The parameters a and b are chosen as $a = 1$, $b = \frac{\pi}{2}$ and, like before, our goal is to go from downright to upright position following the control strategy in Section 6.1. Preliminary simulations reveal that a too high torque by the actor is required to go directly from downright to upright position. To solve this problem we produce a similar curve as the one in Fig. 6.3 and start somewhere outside this curve. A square wave with appropriate amplitude (1 Nm) and

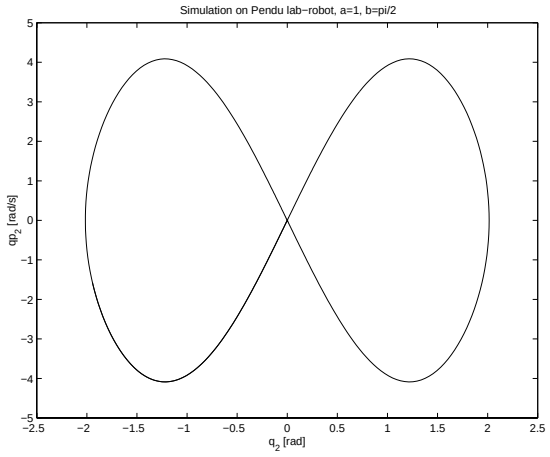

Figure 7.3:

frequency (1 Hz)[1] is set to drive the system until it, (hopefully) at some point in time force the system to a *point* outside this curve. At that point we switch to our zero-dynamical controller discussed in Section 6.1, which will force the system into the zero-dynamics and hopefully to an *orbit* outside the curve. The control block in Fig. 7.2 thus has the following structure

[1]Results in [16] reveals a resonant frequency close to 1 Hz for link 2.

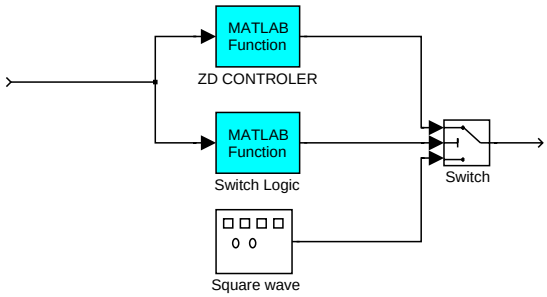

Figure 7.4:

7.3 Experiments

7.3.1 A more robust controller

Executing the control schedule discussed in previous section and estimating the velocities by taking the derivative of the angle measurements with post filtering[2] the common scenario which is presented in Fig. 7.6 appeared. This failure is presumably due to model uncertainty, friction and observer errors. To be able to cope with friction and model uncertainty we need to construct a more robust controller. The friction at each joint is modelled as

$$\begin{cases} d_{11}\ddot{q}_1 + d_{12}\ddot{q}_2 + h_1 = \tau_1 + \Gamma_1 \\ d_{21}\ddot{q}_1 + d_{22}\ddot{q}_2 + h_2 = \Gamma_2 \\ \Gamma_i = \Gamma_{Ci} sgn(\dot{q}_i) + \Gamma_{Vi}\dot{q}_i \end{cases} \tag{7.1}$$

With Γ_{Ci} and Γ_{Vi} representing coulomb and viscous friction coefficients, respectively. Solving for $\ddot{q}_1$ and using $\bar{d}$ and $\bar{h}$ from (6.3) we have

$$\bar{d}\ddot{q}_1 + \bar{h} + \frac{d_{12}}{d_{22}}\Gamma_2 - \Gamma_1 = \bar{d}\ddot{q}_1 + \bar{h} + \bar{\Gamma} = \tau_1 \tag{7.2}$$

Introducing $e_1 = q_1^d - q_1$, $e_2 = \dot{e}_1$, and Δ_1, Δ_2 as general non-linear functions and using the following control law based on estimations of $\bar{d}$, and $\bar{h}$ (denoted $\widehat{\bar{d}}$ and $\widehat{\bar{h}}$), and which is an extension of (6.4)

$$\tau_1 = \widehat{\bar{d}}\nu + \widehat{\bar{h}} + \Delta_2 = \widehat{\bar{d}}(\ddot{q}_1^d + k_1 e_1 + k_2 e_2 + \Delta_1) + \widehat{\bar{h}} + \Delta_2 \tag{7.3}$$

so that $\ddot{q}_1$ becomes

$$\begin{array}{rcl} \ddot{q}_1 & = & \frac{1}{d}(\widehat{\bar{d}}\nu + (\widehat{\bar{h}} - \bar{h}) - \bar{\Gamma} + \Delta_2) = \\ & = & \frac{1}{d}(\widehat{\bar{d}}(\ddot{q}_1^d + k_1 e_1 + k_2 e_2 + \Delta_1) + (\widehat{\bar{h}} - \bar{h}) - \bar{\Gamma} + \Delta_2) \end{array} \tag{7.4}$$

[2] $\dot{q} = (\frac{1-z^{-1}}{h})(\frac{1+z^{-1}+z^{-2}}{3})q$

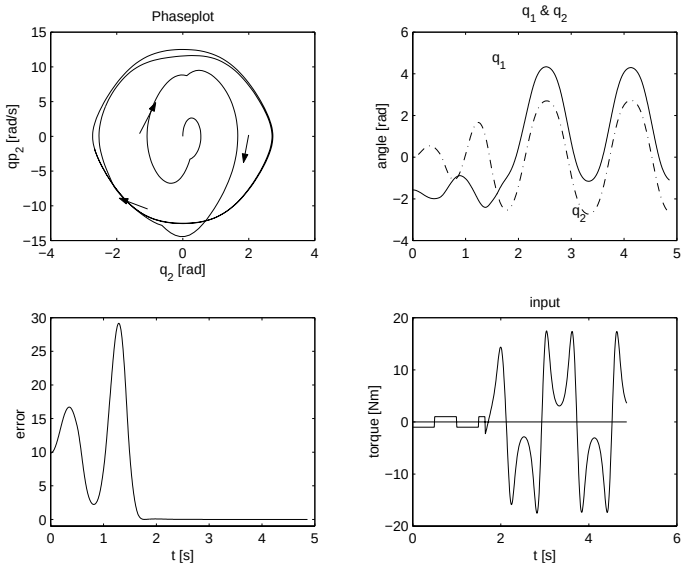

Figure 7.5: Simulation of Pendu lab-robot. Note that error starts to decrease exponentially at $t \approx 1.7$, the same moment as the zero-dynamical controller is switched on which in this case was chosen when $|q_2| > 2.1$ in accordance to the curve in Fig. 7.3. $\omega = 5$, $\xi = 1$.

A more robust controller can be designed by choosing the functions Δ_1 and Δ_2 appropriately as shown by studying the following Lyapunov function candidate based on the error. c_1 and c_2 are constants.

$$\begin{aligned} V &= \tfrac{1}{2}(c_1 e_1^2 + c_2 e_2^2) \\ \dot{V} &= c_1 e_1 \dot{e}_1 + c_2 e_2 \dot{e}_2 = c_1 e_1 e_2 + c_2 e_2 (\ddot{q}_1^d - \ddot{q}_1) = \\ &= c_1 e_1 e_2 + c_2 e_2 (\ddot{q}_1^d - \frac{\widehat{\bar{d}}}{\bar{d}}(\ddot{q}_1^d + k_1 e_1 + k_2 e_2 + \Delta_1) - \frac{(\widehat{\bar{h}} - \bar{h})}{\bar{d}} + \frac{\bar{\Gamma} - \Delta_2}{\bar{d}}) = \\ &= (c_1 - k_1 \frac{\widehat{\bar{d}}}{\bar{d}}) e_1 e_2 + c_2 e_2 ((1 - \frac{\widehat{\bar{d}}}{\bar{d}}) \ddot{q}_1^d - \frac{(\widehat{\bar{h}} - \bar{h})}{\bar{d}}) - c_2 k_2 \frac{\widehat{\bar{d}}}{\bar{d}} e_2^2 - c_2 \frac{\widehat{\bar{d}}}{\bar{d}} \Delta_1 e_2 + \frac{\bar{\Gamma} - \Delta_2}{\bar{d}} c_2 e_2 \end{aligned}$$

If we had a perfect model $\widehat{\bar{d}}/\bar{d} = 1$ and $\widehat{\bar{h}} - \bar{h} = 0$ and all the troublesome terms vanish. Assuming $\widehat{\bar{d}}$ and $\bar{d}$ are of the same sign, a more robust controller can be implemented by on the one hand increasing k_2 by e.g. gain scheduling and on the other by using a sliding mode controller as

$$\Delta_1 = \mu sgn(e_2), \quad \mu > 0 \tag{7.5}$$

We also see that the controller would become even better if we had some model of the friction and by choosing $\Delta_2 = \bar{\Gamma}$.

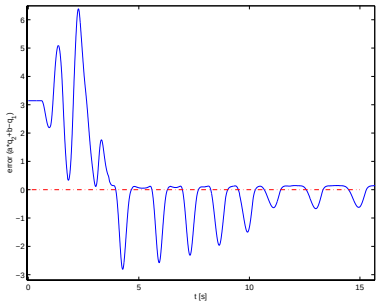

Figure 7.6: From the error plot it is clear that the used controller is not able to keep the system in the zero-dynamics.

7.3.2 Friction estimation

To estimate the friction the following system of linear equations are built up

$$\begin{cases} \ddot{q} = D^{-1}(q)((\tau + \Gamma) - C(q,\dot{q})\dot{q} - G(q)) \\ \\ \ddot{q}_1 = f(q,\dot{q},\tau) = \Gamma_1 f_1(q,\dot{q}) + \Gamma_2 f_2(q,\dot{q}) + f_3(q,\dot{q},\tau) \\ \ddot{q}_2 = g(q,\dot{q},\tau) = \Gamma_1 g_1(q,\dot{q}) + \Gamma_2 g_2(q,\dot{q}) + g_3(q,\dot{q},\tau) \end{cases}$$

$\Leftrightarrow$

$$\begin{cases} \ddot{q}_1 = \Gamma_{C1} sgn(\dot{q}_1) f_1 + \Gamma_{V1}\dot{q}_1 f_1 + \Gamma_{C2} sgn(\dot{q}_2) f_2 + \Gamma_{V2}\dot{q}_2 f_2 + f_3 \\ \ddot{q}_2 = \Gamma_{C1} sgn(\dot{q}_1) g_1 + \Gamma_{V1}\dot{q}_1 g_1 + \Gamma_{C2} sgn(\dot{q}_2) g_2 + \Gamma_{V2}\dot{q}_2 g_2 + g_3 \end{cases}$$

$\Leftrightarrow$

$$\begin{cases} \int \ddot{q}_1 dt = \Gamma_{C1} \int sgn(\dot{q}_1) f_1 dt + \Gamma_{V1} \int \dot{q}_1 f_1 dt + \Gamma_{C2} \int sgn(\dot{q}_2) f_2 dt + \Gamma_{V2} \int \dot{q}_2 f_2 dt + \int f_3 dt \\ \int \ddot{q}_2 dt = \Gamma_{C1} \int sgn(\dot{q}_1) g_1 dt + \Gamma_{V1} \int \dot{q}_1 g_1 dt + \Gamma_{C2} \int sgn(\dot{q}_2) g_2 dt + \Gamma_{V2} \int \dot{q}_2 g_2 dt + \int g_3 dt \end{cases}$$

Making a number of experiments with different input sequences, the problem of finding the friction parameters are reduced to solve the following over determined least-square problem. Integral expressions are left out for simplicity.

$$\begin{pmatrix} \int(\dots)dt \\ \int(\dots)dt \\ \vdots \\ \int(\dots)dt \end{pmatrix} = \begin{pmatrix} \int(\dots)dt & \int(\dots)dt & \int(\dots)dt & \int(\dots)dt \\ \int(\dots)dt & \int(\dots)dt & \int(\dots)dt & \int(\dots)dt \\ \vdots & \vdots & \ddots & \vdots \\ \int(\dots)dt & \int(\dots)dt & \dots & \int(\dots)dt \end{pmatrix} \begin{pmatrix} \Gamma_{C1} \\ \Gamma_{V1} \\ \Gamma_{C2} \\ \Gamma_{V2} \end{pmatrix}$$

This identification approach was executed by doing identification closely around the downright equilibrium position, disturbing the equilibrium with a PRBS signal. The velocities were estimated using an observer, designed by linearizing around the equilibrium and using pole-placement techniques. It turned out that no consistent values could be estimated for the friction parameters at joint two. Most presumably the friction coefficients are close to zero. The friction coefficients belonging to joint one were found to be approximately $\Gamma_{C1} = -0.25\ Nm$ and $\Gamma_{V1} = -0.01\ Nms$ respectively.

7.3.3 A swing up

Implementing the more robust controller discussed in Sec. 7.3.1 resulted in a similar case as the one presented in Fig. 7.6 but with slightly less error amplitude, thus improving performance insignificantly or none at all.

However at some instances it happens that the error is close enough to zero at the same instance q_1 is close enough to $q_1 = \frac{\pi}{2}$ and thus in the region of attraction for the balancing controller. Below such a case is presented

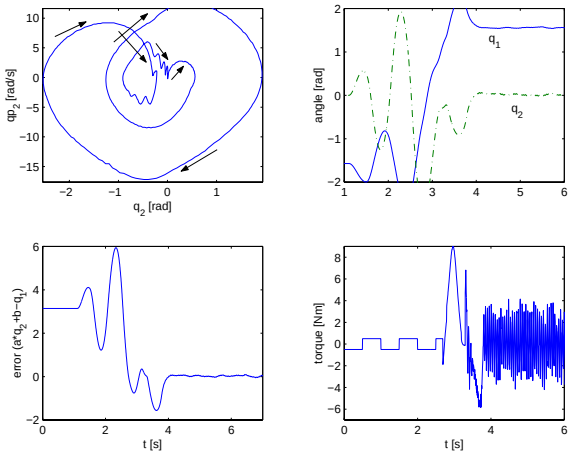

Figure 7.7: An example of a successful swing up for the lab-Pendubot.

Chapter 8

Conclusions

We were not able to prove stability for the zero-dynamical systems, but we can conclude that by stability, periodicity would follow. Several trials to prove stability were presented, involved with finding a Lyapunov function.

A method to force the full system into the zero-dynamics was presented, and we showed how to use this to get the Pendubot to its inverted position. The disadvantage is that there is no way to decide which zero-dynamical orbit the system will take. Also we need a high bandwidth which requires high torques.

Most of the results obtained are only valid for the Pendubot, this because of the strong non-linearities of the Acrobot. Hence this work turned out to be, more or less, a study of the Pendubot zero-dynamics.

Chapter 9

Discussion

What should or shouldn't have been done? There should have been attempts to, in some way, validate the attained friction coefficients. Also a full system identification could have been done to some how eliminate some possible inconsistencies between the friction estimation and the system parameters estimation $(J_1,\ J_2\ ,\ ..., J_5)$, which was not done in this project.

It should also be mentioned that swinging up the lab Pendubot is highly non-repetitive. The fact that it turned out to be very difficult to keep the system in the zero-dynamics is presumably due to model and observer errors. Roughly estimating the bounds of $\widehat{\bar{d}}$ and the "worst case" sign of $(\widehat{\bar{d}}/\bar{d})$ in Sec. 7.3.1 reveals that in some cases sign of $\widehat{\bar{d}}/\bar{d} < 0$ and thus the "robust controller" is no longer robust.

It should also be made clear that for all results obtained no analytic proofs have been discovered and none of the set up goals have been accomplished. The idea was to first prove stability and periodicity of the zero-dynamics and secondly (continuously) changing the parameters a and b in a desired way so to produce walking like gait patterns. A second thought reveals that changing a and b would impose a far more complicated and different sets of zero-dynamical equations than were used.

A perhaps dangerous issue to mention, as it might not be the case, that not taking impact into consideration somehow make the possible use of this study void if the aim is to use it in connection with producing gait patterns, which was the idea.

Chapter 10

Acknowledgements

I would like to write some lines to express my gratitude and esteem for people and friends...old ones, and new ones...

In France: Tan Kok Kong, Pascal Billot, Juan-Carlos Avilla, Rachid Doghmi, Mourad Abed, Ouadi Radouane, Daoser Farsi, Muhammmed "Le Fou", Muhammed Faysal, Kamal Al-Masri and especially Laurent Vallin, Bassam Kattan, Ahmed & Roro Al-Qalalaat, Khodder Melhem and Fadi Al-Masri.

In Sweden: Malek Al-Kasrawi, Christina Grossmann, Rolf Johansson, Magnus Gävfert, and my beloved family members...

Thank you/Merci

And to whom not enough many thanks could be contributed

Alhamduillahi...

Appendix A

Useful theorems

A.1 Lyapunov's stability theorem

Let $x = 0$ be an equilibrium point for $\dot{x} = f(x)$. Let $V : D \to R$ be a continuously differentiable function on a neighborhood D of $x = 0$, such that

$$V(0) = 0 \text{ and } V(x) > 0 \text{ in } D - \{0\}$$
$$\text{and}$$
$$\dot{V}(x) \leq 0 \text{ in } D$$

Then $x = 0$ is stable. Moreover, if

$$\dot{V}(x) < 0 \text{ in } D - \{0\}$$

then $x = 0$ is asymptotically stable.
Proof contained in [1] p 100ff.

A.2 LaSalle's theorem

Lemma *If a solution $x(t)$ of $\dot{x} = f(x)$ is bounded for $t \geq 0$, then its positive limit set L^+ is a nonempty, compact, invariant set. Moreover, $x(t) \to L^+$ as $t \to \infty$.*

Let Ω be a compact (closed and bounded) set with the property that every solution of $\dot{x} = f(x)$ which starts in Ω remains for all future time in Ω. Let $V : \Omega \to R$ be a continuously differentiable function such that $\dot{V}(x) \leq 0$ in Ω. Let E be the set of all points in Ω where $\dot{V}(x) = 0$. Let M be the largest invariant set in E. Then every solution starting in Ω approaches M as $t \to \infty$.
Proof, see [1] p 115.

A.3 Poincaré-Bendixson theorem

Let $\gamma^+(y) = \{\phi(t, y) \mid 0 \leq t \leq \infty\}$ where $\phi(t, y)$ denotes the solution of $\dot{x} = f(x)$, also let γ^+ be bounded and L^+ be its positive limit set. If L^+ contains no equilibrium points, then it is a periodic orbit. Proof, see [1] p 290.

A.4 Criteria for a periodic orbit

From [1] p 299.

- (i) The index of a node, focus or a center is $+1$.
- (ii) The index of a (hyperbolic) saddle is -1.
- (iii) The index of a closed orbit is $+1$.
- (iv) The index of a closed curve not encircling and equilibrium points is 0.
- (v) The index of a closed curve is equal to the sum of the indices of the equilibrium points within it.

Inside any periodic orbit γ there must be at least one equilibrium point. Suppose the equilibrium points inside γ are hyperbolic, then if N is the number of nodes and foci and S is the number of saddles, it must be that $N - S = 1$.

Bibliography

[1] Hassan K. Khalil. *Nonlinear systems [2nd ed.].* Prentice-Hall, 1996.

[2] M.W.Spong, M.Vidyasagar. *Robort Dynamics and control.* John Wiley & Sons, 1989.

[3] M.Reyhanoglu,A van der Schaft, N.H.McClamroch, I.Kolmanovsky. *Nonlinear Control of a Class of Underactuated Systems.* In Proc 35th Conf Decision Contr. pp1682-1687, Kobe, Japan, 1996 .

[4] M.W.Spong. *Underactuated Mechanical Systems.* Lecture Notes in Control and Information Sciences 230 Spinger-Verlag, London, UK, 1997.

[5] A.Isodori. *Nonlinear Control Systems.* Springer-Verlag, Berlin, Germany, 1989.

[6] I.Fantoni, R.Lozano, M.W.Spong. *Energy Based Control of the Pendubot.* IEEE Transaction on Automatic Control. VOL. 45, NO. 4, April 2000.

[7] M.W.Spong. *The swing up control of the Acrobot.* IEEE Int. Conf. Robot. Automat., 1994.

[8] M.W.Spong. *Energy Based Control of a Class of Underactuated Mechanical Systems.* Proccedings of IFAC World Congress, pp31-52, San Francisco, USA 1996.

[9] Ph.Mullhaupt, B.Srinivasan, D.Bonvin. *On the Nonminimum-phase Characteristics of Two-link Underactuated Mechanical Systems.* In Proc 37th Conf on Decision and Contr. Tampa, Canada, 1998 .

[10] T.McGeer. *Passive Walking with Knees.* In Proc. 1990 IEEE Int. Conf. on Robotics and Automation, Los Alamitos, CA, 1990.

[11] D.J.Block. *Mechanical Design and Control of the Pendubot.* Master's Thesis, Univ. Illiois, Urban-Champaign, 1996.

[12] J.Hauser, C.C.Chung. *Converse Lyapunov functions for exponentially stable periodic orbits.* Systems & Control Letters 23, 27-34, 1994.

[13] T.McGeer. *Passive dynamic walking.* Int J. robotics res, April 1990.

[14] Y.Hurmuzlu. *Dynamics and Control of Bipedal Robots.* Control Problems in Robotics and Automation, Springer, 1998.

[15] D.A.Winter. *The Biomechanics and Motor Control of Human Gait: Normal, Eldery and Pathological.* University of Waterloo Press, Onatario, second edition, 1991.

[16] F.M.Bernardi, A.Harryson, M.Zirn. *Identification and control of the Pendubot.* Project in System Identification, Lund Institute of Technology, Departement of Automatic Control, 1999.

[17] R.Johansson. *System Modeling and Identification.* Prentice-Hall, 1993.